Published in final edited form as:

*Cell Rep*. 2016 July 19; 16(3): 744–756. doi:10.1016/j.celrep.2016.06.019.

# Activation of CDK4 triggers development of Non-Alcoholic Fatty Liver Diseases

**Jingling Jin**[3], **Leila Valanejad**[1], **Thuy Phuong Nguyen**[1], **Kyle Lewis**[1,3], **Mary Wright**[1], **Ashley Cast**[1], **Lauren Stock**[2], **Lubov Timchenko**[2], and **Nikolai A. Timchenko**[1,3,*]

[1]Cincinnati Children's Hospital Medical Center, Division of Pediatric General and Thoracic Surgery, 3333 Burnet Avenue ML 7015, Cincinnati, OH 45229

[2]Cincinnati Children's Hospital Medical Center, Department of Neurology, 3333 Burnet Avenue ML 7015, Cincinnati, OH 45229

[3]Baylor College of Medicine, Huffington Center on Aging, One Baylor Plaza, Houston Texas, 77030

## Summary

The development of Non Alcoholic Fatty Liver Disease (NAFLD) is a multiple step process. Here we show that activation of cdk4 triggers the development of NAFLD. We found that cdk4 protein levels are elevated in mouse models of NAFLD and in patients with fatty livers. This increase leads to C/EBPα phosphorylation on Ser193 and formation of C/EBPα-p300 complexes, resulting in hepatic steatosis, fibrosis, and HCC. The disruption of this pathway in cdk4-resistant C/EBPα-S193A mice dramatically reduces development of high fat diet (HFD)-mediated NAFLD. In addition, inhibition of cdk4 by flavopiridol or PD-0332991 significantly reduces development of hepatic steatosis, the first step of NAFLD. Thus, these studies reveal that activation of cdk4 triggers NAFLD, and that inhibitors of cdk4 may be used for the prevention/treatment of NAFLD.

## Graphical Abstract

*Correspondent author: Nikolai A. Timchenko, Cincinnati Children's Hospital Medical Center, Division of Pediatric General and Thoracic Surgery, 3333 Burnet Avenue ML 7015, Cincinnati, OH 45229. Phone: 513-636-0129, Nikolai.Timchenko@cchmc.org. Jingling Jin, Leila Valanejad and Thuy Phuong Nguyen contributed equally to this work.



**Author Contributions**

JJ and KL designed and performed experiments with examination of NAFLD in C/EBPα-S193A and C/EBPα-S193D mice. TPN, LV, MW and AC designed and performed experiments with prevention and treatments of HFD-mediated hepatic steatosis by inhibitors of cdk4. LS and LT designed and performed ITT test and examined expression of glucose and lipogenic enzymes. NT generated the ideas and supervised all studies. NT, JJ, TPN, LT and LV wrote the paper.

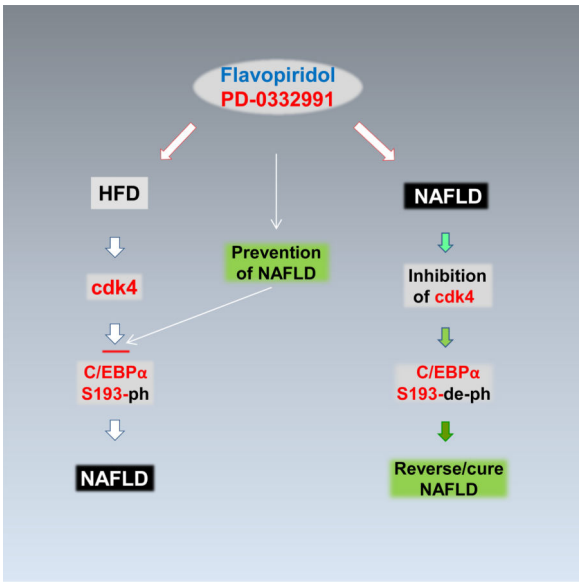


**Keywords**

cdk4; cyclin D3; NAFLD; p300; C/EBP; hepatic steatosis

## Introduction

NAFLD generally develops under conditions of high fat diet and aging as the disease progresses over several stages. The first stage is the development of hepatic steatosis, which is characterized by an accumulation of triglycerides (TG) in the cytoplasm of hepatocytes. Hepatic steatosis can further progress to non-alcoholic steatohepatitis (NASH) and ultimately to cirrhosis and hepatocellular carcinoma (HCC) if not treated or prevented (Cohen et al., 2011; Hebbard and George, 2011). With advanced age, patients develop hepatic steatosis and have an increased risk in developing liver cancer (Schmucker, 2005; Timchenko, 2011). Accumulation of fat in the liver (hepatic steatosis) might be a result of multiple alterations of fat metabolism, including enhanced fat up-take, increased lipogenesis, and decreased secretion of very low-density lipoproteins (Cohen et al., 2011). C/EBPα and C/EBPβ are two members of the C/EBP family. Members of this protein family contain a basic region and a leucine zipper region (Johnson, 2005) and dimerize and control multiple functions in different tissues. C/EBPα is required for liver differentiation, where it acts as a strong inhibitor of liver proliferation (Timchenko, 2009; Wang et al., 2006). The biological activities of C/EBPα are mainly controlled by post-translational modifications. Among several important modification sites is Ser193, a key amino acid of C/EBPα through which multiple functions of C/EBPα are regulated, including its role in the biology of the liver (Wang and Timchenko, 2005; Jin et al., 2010; Wang et al., 2010). It has been shown that cyclin D3-cdk4 phosphorylates C/EBPα on Ser193 causing C/EBPα to associate with the chromatin remodeling protein p300. C/EBPα-p300 complex formation results in alterations of chromatin structure (Jin et al., 2010) that, in turn, leads to C/EBPα–dependent growth

arrest (Wang et al., 2010, Jin et al., 2010). Our recent paper (Jin et al., 2013) showed that phosphorylation of C/EBPα at Ser193 regulates steatosis.

Cyclin-dependent kinase 4 (cdk4) is an important regulator of C/EBPα activity. Cdk4 is activated by D-type cyclins (D1, D3, and D3) and mediates progression of the cell cycle through G1 phase by phosphorylation of retinoblastoma protein (Rb) and subsequent release of Rb-dependent repression of S-phase genes (Baker & Reddy, 2013). Cdk4 and cdk6 are highly homologous and share many properties. Therefore, the majority of the information about cdk6 also applies to cdk4. Crystal structures of the p16-cdk6 complexes revealed that p16 interacts with amino acid residues located in the active sites of cdk4 and cdk6 and diminishes kinase activities of cdk4 and cdk6 (Gil & Peters, 2006; Endicot et al., 1999). A systematic screen for cdk4/cdk6 substrates in HEK293 cells identified a broad number of substrates (Anders et al., 2011). Since cdk4 is involved in the development of cancer, cdk4 inhibition is under intensive investigation for cancer therapy. The initial development of cdk4/6 inhibitors led to the discovery of the first generation of inhibitors such as flavopiridol and roscovitine (Dickson and Schwarz, 2009). Further search for more specific and non-toxic inhibitors has identified a small compound, PD-0332991, which seems to be the best inhibitor of cdk4/6. It has been shown that PD-0332991 causes G1 growth arrest by blocking phosphorylation of Rb (Rivadeneira et al., 2010).

In this paper, we found that the triggering event in the development of HFD-mediated NAFLD is the elevation of cdk4 and subsequent promotion of C/EBPα-p300 complexes. Disruption of this pathway by genetic mutation of C/EBPα and by inhibition of cdk4 significantly inhibits the development of NAFLD.

## RESULTS

### Cdk4 is activated by HFD and phosphorylates C/EBPα at Ser193 leading to an increase of C/EBPα-p300 complexes

We have previously shown that the elevation of C/EBPα-p300 complexes is involved in development of hepatic steatosis. Since cdk4 phosphorylates Ser193 and increases the formation of C/EBPα-p300 complexes (Jin et al., 2013), we examined if cdk4 is activated in WT mice during development of NAFLD under HFD conditions. WT mice were treated with HFD for 3 and 12 weeks, livers were harvested and examined for the expression of proteins of the cyclin D3-cdk4-C/EBP-p300 pathway. Representative results are shown in Fig 1A. We found that both cyclin D3 and cdk4 are elevated at 3 and 12 weeks of HFD and that this elevation leads to increased phosphorylation of C/EBPα at Ser193. Co-IP studies showed that amounts of C/EBPα-p300 complexes are increased in livers of mice at 3 and 12 weeks of HFD (Fig. 1B). Note that levels of C/EBPα, C/EBPβ and p300 are also increased at 3 and 12 weeks of HFD. However, these proteins form a tripartite complex only if C/EBPα is phosphorylated at Ser193 (Jin et al., 2013; 2015). Based on these data, we hypothesized that cdk4 is a key protein which increases C/EBPα-p300 complexes under conditions of HFD in mice leading to NAFLD.

### Cdk4-C/EBPα-p300 pathway is activated in patients with NAFLD

Given activation of cdk4-C/EBPα-p300 in HFD-mediated NAFLD in mice, we next asked if this pathway is activated in livers of patients with NAFLD. Western blotting with nuclear extracts isolated from control livers and from livers of NAFLD patients showed that cdk4 is significantly increased in NAFLD patients (Fig 1C). Calculation of cdk4 as a ratio to β-actin revealed that cdk4 is 6–8 fold elevated in livers of patients with NAFLD. We have next examined cdk4 expression in two control livers and in 4 livers from patients with NAFLD using immunostaining approaches. This assay showed that cdk4 is increased in all examined samples from patients with fatty liver disease (Fig 1D). We have previously shown that human C/EBPα is phosphorylated at Ser190 in the livers of these patients (Jin et al., 2013). Therefore, we next examined if this phosphorylation might result in the formation of C/EBPα-p300 complexes using Co-IP approach. We found that amounts of these complexes are increased in livers of NAFLD patients (Fig 1E). Because the C/EBPα-p300 complexes activate promoters of enzymes of TG synthesis, we examined expression of key enzymes GPAT and DGAT2 which catalyze the first and the last steps of TG synthesis. Figure 1F shows that expression of both enzymes is increased in livers of patients with NAFLD. Thus, these studies demonstrated that cdk4-C/EBPα-p300 pathway is activated in patients with NAFLD and correlates with elevation of enzymes of TG synthesis. From the results obtained in mice and data collected in humans, we hypothesized that cdk4 might be a key, triggering, event in the development of hepatic steatosis and further stages of NAFLD (Fig 1G).

### HFD-mediated hepatic steatosis is inhibited in cdk4-resistant S193A mice

To examine if cdk4-dependent phosphorylation of C/EBPα at Ser193 is involved in the development of NAFLD, we have utilized two knock-in mouse models: constitutively active C/EBPα-S193D mice (Wang et al., 2010; Jin et al., 2010) and recently generated cdk4-resistant C/EBPα-S193A mice (Jin et al., 2015). Due to the fact that C/EBPα cannot be phosphorylated at Ser193 by cdk4 in S193A mice, we first examined if these mice expressing cdk4-independent C/EBPα might be resistant to the development of hepatic steatosis in a short time frame of HFD protocol. We have treated S193A mice with HFD for 3 and 12 weeks. An identical treatment was performed with S193D mice and with WT mice as the controls. Figure 2A shows H&E and Oil Red-O staining of livers under normal diet (ND) and 3 and 12 weeks of HFD. In agreement with previous observations, WT mice develop steatosis at 3 and 12 weeks while S193D mice have much stronger steatosis at the same time points. In S193A mice, however, both H&E and Oil-Red-O staining showed no steatosis at 3 weeks and a much weaker steatosis at 12 weeks. These data indicate that knock-in mice expressing the cdk4-resistant C/EBPα-S193A mutant are also resistant for development of hepatic steatosis within 12 weeks of HFD. Since steatosis is inhibited in S193A mice and because these mice have reduced basal levels of glucose (Jin et al., 2013), we asked if these animals might have changes in insulin sensitivity. Therefore, we have performed Insulin Tolerance Test (ITT); however, no differences were detected in insulin sensitivity between WT and S193A mice. Insulin mediated glucose-lowering was identical in both groups (Fig 2B). Note that, while the ITT test shows the reduction of the glucose as percentage to the levels observed before insulin injection, the levels of glucose were lower in S193A mice during the entire duration of the test (Supplemental Figure 1).

### Cdk4-resistant S193A mice do not accumulate C/EBP p300 complexes

We next determined a molecular basis for the resistance of S193A mice to develop steatosis. We first examined if cdk4 and cyclin D3 are properly activated in S193A mice. Similar to WT mice, both these proteins are increased in livers of S193A mice at 3 and 12 weeks of HFD (Fig 2C and E). Examination of C/EBPα and p300 proteins also showed that they are elevated in WT and S193A mice at 3 and 12 weeks with a slightly lower elevation in S193A mice. In agreement with observations shown in Fig 1A–B, co-immunoprecipitation studies revealed that C/EBPα-p300 complexes are elevated in WT mice; however, these complexes are not detectable in livers of S193A mice after HFD treatments (Fig 2C). These studies clearly demonstrated that the mutation of S193 to Ala blocked the formation of C/EBPα-p300 complexes in the animals under HFD protocol.

### The lack of C/EBPα-p300 complexes resulted in failure of S193A mice to activate enzymes of TG synthesis and enzymes of glucose synthesis

Our previous studies have shown that C/EBPα-p300 complex is a positive regulator of enzymes of triglyceride synthesis GPAT and DGAT1/2 (Jin et al., 2013) and enzymes of glucose synthesis PEPCK and G6-phase (Jin et al., 2015). The reduction of G6-phase in S193A mice has been also recently published (Fleet et al., 2015). Since these proteins are key regulators of hepatic steatosis, we asked if their levels might be changed in livers of S193A mice under conditions of HFD protocol. We found that GPAT, DGAT1, DGAT2, PEPCK and G6-phase are elevated in livers of WT mice at 3 and 12 weeks of HFD; however, no elevation of these proteins was detected in livers of S193A mice (Fig 2D). Since GPAT, DGAT1 and DGAT2 are key enzymes of TG synthesis, the failure of activation of these proteins by p300-C/EBPα complexes in S193A mice seems to be the main mechanism of the inhibition of hepatic steatosis. To further examine if other lipogenic pathways are altered in S193A mice, we examined expression of FASN, ACC and SCD by Western blotting and found that these lipogenic pathways are activated in livers of WT mice at 3 and 12 weeks, but livers of S193A mice do not increase expression of these proteins (Fig 2D). Thus, these studies revealed that cdk4-resistant S193A mice do not develop hepatic steatosis under HFD protocol and that this correlates with a failure to form the C/EBPα-p300 complexes and to activate genes which are involved in development of hepatic steatosis.

### Development of HFD-mediated fibrosis is inhibited in S193A mice

It has been shown that long term treatments of mice with HFD lead to further development of NAFLD including progression to fibrosis, cirrhosis and HCC. Therefore, we next examined if the disruption of cdk4-C/EBPα pathway in S193A mice might affect the development of fibrosis under a HFD protocol. Previous studies showed that fibrosis is very well developed in mouse livers at 6–7 months after initiation of HFD protocol (Hill-Baskin et al., 2009). Therefore, we fed WT, S193D and S193A mice with high fat diet for 7 months and examined fibrosis using several approaches. H&E and Oil-Red-O staining showed that while WT and S193D mice have significant accumulation of fat droplets, the development of hepatic steatosis is weaker in S193A mice (Fig 3A). Examination of livers under a higher magnification showed that there are detectable differences in the liver structure (Fig 3B). We

next examined development of fibrosis by staining livers with Sirius Red and found that development of fibrosis is significantly inhibited in S193A mice (Fig 3A).

### C/EBPα-S193A mice have reduced hepatic steatosis at 12 months of HFD

We next examined the development of NAFLD in S193A mice after very long treatments with HFD. For this goal, 5 mice of each genotype were treated with HFD for 48 weeks (12 months). All animals survived these long treatments, but WT and S193D mice were fatty and, as expected, developed liver disease. H&E staining showed that S193D mice have developed severe macrovesicular steatosis and that liver architecture was significantly destroyed with significant loss of hepatocytes (Figure 3C). Livers of WT mice also have developed these disorders but to a less degree. On the contrary to these two mouse lines, S193A livers had much less steatosis and relatively abundant hepatocytes (Fig 3C). Oil-Red-O staining confirmed that development of steatosis is inhibited in S193A livers after 12 months of HFD protocol. Examination by α-SMA staining showed that development of fibrosis is also inhibited in S193A mice (Fig 3C).

### NAFLD is reduced, but liver proliferation is increased in S193A mice after 12 months of HFD

The 12 months duration of HFD protocol usually initiates development of liver cancer. One of the characteristics of liver cancer is increased liver proliferation. To examine the degree of liver proliferation in our animal models, we performed a set of studies using several approaches. First, we calculated number of mitotic figures and found that all three mouse models have increased mitosis after 12 months of HFD, but the level of mitosis is different. Despite higher steatosis, the mitosis in S193D mice was lower than in WT mice. On the contrary, cdk4-resistant S193A mice had higher levels of proliferation, but much less steatosis (Fig 4A and B). Second, we performed ki67 staining and found that proliferation of S193A hepatocytes is significantly higher than one of WT livers, while S193D mice have reduced number of ki67-positive hepatocytes (Fig 4A and B). These results are consistent with growth inhibitory/tumor suppression activities of C/EBPα mutants S193D and S193A (Wang et al., 2010; Jin et al., 2015) and suggest that S193D mutant inhibits liver proliferation under HFD protocol; while S193A does not. We next examined expression of cdk4 and phosphorylation status of C/EBPα in our animal models after 7 and 12 months of HFD treatments. In these studies, we have incorporated protein extracts of 3 months HFD-treated mice. Figure 4D shows that cdk4 is activated in all three mouse lines and that C/EBPα is phosphorylated at Ser193 in WT mice, but not in S193A mice. Interestingly, ph-S193 specific antibodies also recognized S193D mutant, which is reduced at 12 month of HFD in livers of S193D mice. Examination of cyclin A as an indicator of proliferation revealed that cyclin A is increased in all mouse lines at 7 and 12 months of HFD. In these studies, we found that cyclin A is also activated in WT mice after 3 months of HFD protocol. To examine intracellular localization of cdk4 after 12 months of HFD, we immunostained livers of WT mice with antibodies to cdk4. This assay confirmed that cdk4 is significantly increased in livers of HFD-treated mice at 7 and 12 months and that the major fraction of cdk4 is located in nucleus (Fig. 4E).

Our previous observations found that development of liver cancer under conditions of DEN-mediated carcinogenesis is facilitated by a down-regulation of farnesoid X receptor, FXR, and up regulation of an oncogene Gankyrin, Gank (Jiang et al., 2013). To examine if this pathway of liver cancer is initiated after 7 and 12 months of HFD, we used Q-RT PCR approach with mRNA isolated from WT, S193D and S193A mice. In WT mice, we detected a dramatic reduction of FXR at 7 months and a 3-fold reduction at 12 month. In agreement with the role of FXR as a repressor of Gank, the levels of Gank are 2–4 fold elevated in WT mice at 7 and 12 months of HFD. Examination of S193D and S193A mice surprisingly showed that FXR is reduced in both these lines without treatments; but is slightly elevated in S193D and reduced in S193A mice compared to non-treated animals (Fig 4F). However, comparisons to the levels of FXR in WT non-treated mice showed that levels of FXR are reduced in all three mouse lines after 7 and 12 months of HFD protocol. We also found that levels of Gank are elevated in both S193D and S193A mice at 12 months after initiation of HFD protocol (Fig 4F). Taken together, these studies demonstrated that 12 months HFD treatments of all three mouse lines lead to the severe steatosis in WT and S193D mice and that steatosis in inhibited in livers of S193A mice. We also found that liver proliferation is significantly increased and cancer-specific FXR-Gank pathway is activated in all three lines; however, liver proliferation is not strongly activated in S193D mice due to growth inhibitory activity of this mutant.

## Inhibition of cdk4 by flavopiridol prevents development of the first stage of NAFLD, hepatic steatosis

Figure 4G summarizes the examination of HFD-mediated NAFLD in our animal models. Given a strong inhibition of NAFLD in cdk4-resistant C/EBPα-S193A mice, we asked if the inhibition of cdk4 by pharmacological intervention might reduce the development of hepatic steatosis (Fig 4G) in the mice under HFD protocol. In the first set of experiments, we used flavopiridol (FPD) as the inhibitor of cdk4. Note that FPD also inhibits cdk2 (Nagaria et al., 2013; Luke et al., 2012). Control WT mice were treated with HFD; while experimental mice were treated with HFD plus FPD for 5 weeks. Examination of livers by Oil-Red-O staining showed that control mice have developed hepatic steatosis; however, FPD treated mice do not show detectable steatosis (Fig 5A). Examination of enzymes of TG syntheses DGAT1 and DGAT2 showed significant increases in HFD control mice, but no elevation was observed in livers of mice treated with FPD (Fig 5B). To examine if FPD inhibits activity of cdk4, we have performed Western blotting with antibodies to a target of cdk4, ph-780-Rb protein. These studies revealed that HFD-mediated activation of cdk4 leads to significant phosphorylation of Rb and that FPD completely inhibits cdk4 activity; and phosphorylated forms of Rb are not detectable in livers of mice treated with FPD (Fig 5B). We next examined cdk4-C/EBPα-p300 pathway in livers of control and FPD-treated mice. Although our original hypothesis was that the inhibition of cdk4 by FPD might block phosphorylation of C/EBPα and subsequent formation of complexes with p300, we surprisingly found that the inhibition of cdk2/cdk4 by FPD has much broader and much stronger effect on the expression of several components which are involved in the formation of C/EBPα-p300 complexes. Particularly, we observed that FPD inhibits HFD-mediated elevation of cyclin D3, C/EBPα, C/EBPβ and p300 while these proteins are elevated in control HFD treated mice (Fig 5B). In agreement with the reduction of C/EBPα and p300 proteins, we could not

detect C/EBPα-p300 complexes in FPD-treated mice (Fig 5B). Given the unexpected results showing the reduction of protein levels of C/EBP proteins which inhibit liver proliferation, we performed a careful examination of liver proliferation in WT mice. Examination of cell cycle proteins showed activation of cyclin E, cdc2 and cdk2 in control mice treated by HFD; however FPD completely blocked activation of all these proteins (Fig 5C). We next examined number of mitotic figures and number of ki67-positive hepatocytes. In agreement with effects of FPD on cell cycle proteins, we observed that HFD significantly increases mitosis and number of ki67 positive hepatocytes and that FPD blocks this activation (Fig 5D, E and F). Given these unexpected results showing the activation of liver proliferation by a very short treatment (5 weeks) with HFD, we examined if proliferation of the liver was initiated in WT mice at early time points using animals shown in Fig 2. These animals were treated with HFD for 3 and 12 weeks. Ki67 staining revealed that 3 weeks of HFD treatments are sufficient to initiate liver proliferation (Fig 5G). Figure 5H summarizes examination of effects of FPD on HFD-mediated steatosis. We found that HFD induces both liver proliferation by activating cdk2/cdk4 and NAFLD through elevation of p300-C/EBPα complexes. The inhibition of cdk2/cdk4 by FPD blocks development of hepatic steatosis and liver proliferation.

## Inhibition of cdk4 by a more specific inhibitor, PD-0332991, inhibits development of HFD-dependent hepatic steatosis but does not block liver proliferation

Our data for increase of liver proliferation are in agreement with a previous report showing that high fat diet initiates liver proliferation which correlates with inflammatory changes (VanSaun et al., 2013). Our data demonstrated that this elevation of proliferation occurs at very early time points (3 weeks after initiation of HFD protocol, Fig 5G) suggesting that this increase contributes to the further development of steatosis. To address this issue, we utilized a more specific inhibitor of cdk4, PD-0332991 (Flaherty et al., 2012; Leonard et al., 2012), in a similar setting of HFD-mediated steatosis. Note that we used a dose of PD-0332991 much lower than that described in literature. Oil-Red-O staining and Western blotting with antibodies to DGAT1 and DGAT2 revealed that PD-0332991 (given with chow, 150mg/kg chow) prevents development of HFD-mediated hepatic steatosis (Fig 6A and B). To examine if this block of hepatic steatosis is mediated by inhibition of cdk4 activity, we looked on the phosphorylation status of its targets Rb-Ser780 and C/EBPα-S193-ph. Western blotting with specific antibodies showed that both substrates are phosphorylated after treatments with HFD and that inhibition of cdk4 blocks or significantly reduces this phosphorylation (Fig 6B). Co-IP studies revealed that the inhibition of cdk4 and reduction of S193-ph isoform of C/EBPα dramatically reduces C/EBPα-p300 complexes (Fig 6C). We next examined if the inhibition of cdk4 by PD-0332991 blocks liver proliferation using three approaches. Examination of cell cycle proteins, cyclin D1, cyclin D3, cdk2 and cdc2 and counting the number of ki67-positive hepatocytes showed that treatment with PD-0332991 does not prevent the increase of liver proliferation initiated by HFD (Figs 6B, D and F). To get additional support for this result, we examined DNA replication by measuring BrdU uptake and found that PD-0332991 treatment does not inhibit liver proliferation under conditions of our experiments (Fig 6E and G). Figure 6H shows a summary of these studies. We found that HFD-mediated hepatic steatosis and HFD/cdk2–4-mediated increase of liver proliferation are parallel events and that HFD-mediated liver proliferation does not seem to

contribute to the development of hepatic steatosis. These data and the lack of C/EBPα-p300 complexes strongly suggest that the cdk4-C/EBPα-p300 signaling is the main cause of hepatic steatosis.

### Inhibition of cdk4 by PD-0332991 in mice with existing hepatic steatosis reverses NAFLD

Although our data clearly show that inhibition of cdk4 prevents development of hepatic steatosis, the next important question is if the inhibition of cdk4 might reverse existing steatosis. This is quite important because the patients with NAFLD need an approach to cure NAFLD. To test if the treatment with PD-0332991 reverses hepatic steatosis, we applied a strategy shown in Fig 7A. Four groups of mice were used for 5 weeks and 10 weeks duration of the treatments. The first group fed HFD for 5 weeks. The second group fed normal diet; while the third group fed HFD for entire 10 weeks duration of the protocol. The fourth experimental group was fed HFD for the first 5 weeks and then HFD plus PD-0332991 were given for the next 5 weeks. Animals were sacrificed 5 or 10 weeks after initiation of the protocol and hepatic steatosis was examined by Oil-Red-O staining. Figure 7B shows that 5 weeks HFD group developed significant steatosis and that 10 weeks HFD group of mice further developed severe steatosis. However, inhibition of cdk4 by PD-0332991 dramatically reduced steatosis in the fourth group compared to both 5 and 10 weeks HFD groups. Thus, these studies demonstrated that inhibition of cdk4 reverses hepatic steatosis even with continued treatments with HFD. We next examined cdk4-C/EBPα pathway in mice treated for 10 weeks with HFD and HFD plus PD-0332991. Western blotting showed that although protein levels of cdk4 are not reduced by PD-0332991, the activity of cdk4 is dramatically inhibited and Rb is not phosphorylated in mice treated with the inhibitor (Fig 7C). Consistent with Oil-Red-O results, amounts of DGAT1 and DGAT2 proteins are reduced in mice treated with the inhibitor. We next examined C/EBPα-p300 complexes using co-IP approach. Figure 7D shows that C/EBPα-p300 complexes are significantly reduced or are not detectable in mice with inhibited cdk4 activity. These results clearly demonstrate that the PD-0332991-mediated reversal of hepatic steatosis is associated with the inhibition of cdk4 and with subsequent reduction of C/EBPα-p300 complexes. Because HFD also initiates liver proliferation, we asked if reversion of the steatosis by PD-0332991 involves the inhibition of liver proliferation. Three approaches were used: examination of cell cycle proteins cdc2 and cdk2, BrdU up-take and staining with antibodies to ki67. Figure 7C shows that levels of cdk2 and cdc2 are increased by HFD and that the inhibition of cdk4 in mice with existing steatosis does not reduce levels of these proteins. Figure 7E shows typical pictures of BrdU and ki67 staining. Calculations of BrdU-positive and ki67-positive hepatocytes showed that, at the low doses used in our experiments, PD-0332991 did not inhibit liver proliferation in the reversal experiments (Figures 7F and G). Taken together, these studies revealed that PD-0332991-mediated inhibition of cdk4 reverses hepatic steatosis through the disruption of C/EBPα-p300 complexes, but does not affect HFD-mediated proliferation of the liver (Fig 7H).

## Discussion

Recent methodological progress has determined a number of global changes which are associated with NAFLD (Hebbard and George, 2011). Despite this progress, very little is

known about key events causing the development NAFLD. NAFLD in humans is usually associated with age and with use of inappropriate diet which first leads to the development of hepatic steatosis which further progresses into fibrosis, steatohepatitis (NASH) and hepatocellular carcinoma, HCC. One of the best and biologically relevant animal models of NAFLD is the high fat diet treatment of mice. This treatment mimics the main steps of development of NAFLD in humans: hepatic steatosis, fibrosis, NASH, cirrhosis and HCC. Transcription factors of C/EBP family, C/EBPα and C/EBPβ, are key factors that are involved in development of NAFLD. We have previously generated two C/EBPα knock-in mouse models in which Ser193 is mutated to Aspartate (S193D) and to Alanine (S193A). We found that S193D mice develop hepatic steatosis much faster than WT mice due to an elevation of C/EBPα/β-p300 complexes which activate five enzymes of TG synthesis (Jin et al., 2013). This work suggested that there might be a kinase which is activated during development of NAFLD and triggers NAFLD. In this paper, we have identified cdk4 as such kinase, which is activated in mouse models of NAFLD and in patients with fatty liver disease. Our manuscript presents a number of experimental evidence showing that inhibition of cdk4 by specific inhibitors and/or blocking of the phosphorylation of its downstream target C/EBPα by genetic mutation of Ser193 to Ala dramatically inhibits development of NAFLD in animal models. These studies clearly demonstrate that the inhibitors of cdk4 can be considered for the treatments of NAFLD in patients. It is interesting that cdk4 inhibitor PD-0332991 is used in clinical trials for the treatments of patients with liver cancer (Flaherty et al., 2012; Leonard et al., 2012) suggesting that it might be easily used for the treatments of NAFLD patients.

Although the HFD-mediated initiation of liver proliferation has been previously reported (VanSaun et al., 2013), the contribution of the liver proliferation to NAFLD has not been examined. We found that a very short treatment of mice with HFD (3 weeks) is sufficient to initiate liver proliferation. This finding raised the question if liver proliferation might contribute to development of steatosis and further steps on NAFLD. Figures 5H, 6H and 7H summarize our findings and present our hypotheses based on experiments with two inhibitors of cdk2/cdk4 and with genetically modified S193D and S193A mice. We found that increased liver proliferation is not involved in the development of hepatic steatosis. In fact, hepatic steatosis is much stronger in S193D mice, while the proliferation is significantly lower than proliferation in WT and S193A mice (Fig 4A–C). This opposite correlation rather suggests that the increased proliferation in WT mice might be a mechanism by which liver tries to block the development of NAFLD. It is also important to emphasize that our studies identified a new relationship between C/EBPα and FXR. Our results show that FXR is a downstream target of C/EBPα and that FXR is reduced in livers of animal models, S193A and S193D mice (Fig 4). Since many reports revealed that FXR is involved in development of NAFLD (Carr and Reid, 2015; Xu et al., 2014), this finding suggests that cdk4-C/EBPα pathway might also promote NAFLD through regulation of FXR.

The critical finding of our work is identification of a key event in the development of NAFLD which is elevation/activation of cdk4. This finding and further work with inhibitors of cdk4 provide strong support for the consideration of inhibition of cdk4 as a promising possible treatment which prevents liver from development of steatosis and which might

reduce existing steatosis. It is important to note that liver injury is one of the main causes of NAFLD. Our studies of cdk4-resistant C/EBPα-S193A mice showed significant inhibition of liver injury and the inhibition of steatosis at 7 and 12 months of HFD protocol. On the contrary, knockin mice expressing constitutively active C/EBPα-S193D mutant have much more severe liver injury that WT or S193A mice and develop severe steatosis especially at 12 months after initiation of HFD. In experiments with prevention and the reversal of steatosis, we examined if inhibitors of cdk2/cdk4 might prevent/reverse liver injury. However, within duration of these experiments (10 weeks), we did not detect alterations of ALT/AST in WT mice. We also performed TUNEL staining and immunoblotting livers for activated caspase 3. Under conditions of our experiments, these approaches did not detect liver injury within the 10 weeks duration of HFD protocol. On the other hand, our experiments with Sirius Red detected a very minor staining of livers of WT mice treated with HFD for 10 weeks; while this staining was not detected in animals treated with HFD plus PD-0332991 (Supplemental Figure 3). Since the development of HFD-mediated fibrosis/liver injury requires long treatments with HFD (up to 7 months), it would be important to perform long term studies with HFD treatments and test if cdk4 inhibitors might block the development of HFD-mediated fibrosis in this setting. At this stage of investigation, it is important to note that we have previously examined ALT/AST in S193D and S193A mice (Jin et al., 2015; Wang et al., 2010) and found that ALT and AST are elevated in S193D mice; while they are reduced in S193A mice. It is likely that that the less injury in S193A mice in the beginning of HFD protocol might be involved in protection from NAFLD. It is interesting to mention that while we have used relatively low doses of PD-0332991, we detected very strong prevention and reversion of steatosis within the time frame of 10 weeks of HFD treatments. It is also important to mention that, in reversal experiments, we kept feeding HFD and PD-0332991 simultaneously for 5 weeks and, despite HFD, the inhibitor of cdk4 dramatically reduced hepatic steatosis. This study gives great hope that cdk4-based therapy might be a worthy approach to treat patients with NAFLD, at least at early stages of the disease. Further studies with animals are required to test if cdk4 inhibitors might reverse late steps of NAFLD such as fibrosis and NASH. Considering treatments of NAFLD patients with inhibitors of cdk4, it is important to keep in mind that although PD-0332991 is a more specific inhibitor of cdk4, there is a risk of development of liver cancer because it does not inhibit liver proliferation. From this point of view, inhibition of cdk4 by flavopiridol might have a better outcome. In summary, our work elucidated the key event in the HFD-mediated NAFLD and provided the strong support for consideration of cdk4 inhibitors as a possible tool to treat NAFLD.

## Experimental Procedures

### Animals

**High Fat Diet protocol—**Experiments with animals were approved by the Institutional Animal Care and Use Committee at Baylor College of Medicine (protocol AN-1439) and by the IACUC at Cincinnati Children's Hospital (protocol IACUC2014-0042). In this paper, we have used 2–4 month old WT, C/EBPα-S193D mice and C/EBPα-S193A mice. Generation and characterization of C/EBPα-S193D and C/EBPα-S193A mice were described in our previous papers (Wang et al., 2010; Jin et al., 2010; 2013). Livers were harvested and kept at

−80°C. For high fat diet experiments, mice and their age-matched littermate controls were fed either a standard laboratory chow diet or a high-fat diet (D12331, Research Diets, New Brunswick, NJ) for 3 or 12 weeks for a short term study, or for 20 to 48 weeks for long term studies.

**Inhibition of cdk4 by flavopiridol (FPD) and PD-0332991 (PD)—**To inhibit activity of cdk4, we have fed animals with inhibitors in chow diet (custom made by BioServ) ad libitum for 7 days prior initiation of HFD protocol. After the 1-week pre-treatment, mice were given HFD and have been kept on the 0.025% FPD or PD (in chow, 150mg/kg chow) for 4 additional weeks. In the end of experiments, mice were sacrificed and livers were examined for development of hepatic steatosis and for expression of genes as described below. Five mice per each group of the protocol were used. In the reversal studies, we used four groups of mice (5 mice/group, males). The protocol for reversal studies is summarized in Fig 7A.

**Liver histology and immunohistochemistry—**The livers were fixed overnight in buffered 10% formaldehyde, embedded in paraffin, and sectioned at a thickness of 5 μm. The sections were then stained with hematoxylin and eosin using a standard protocol or with different antibodies against cdk4 (C-22, Santa Cruz). For Oil Red O staining of lipid droplets in frozen liver sections, the liver cryosections of 7 μm were stained with by commercially available kits (IW-3008, IHC world). Sirius Red staining was performed using “Direct Red 80” (Sirius Red, Sigma-Aldrich) kit.

**Antibodies and Reagents—**Antibodies to C/EBPβ (C-19), C/EBPα (14AA), DGAT1 (H-255), DGAT2 (H-70), GPAT, PEPCK, G6-phase, p300 (N-15 or C-20), cdk4 (C-22), cyclin D3 (C-16) were from Santa Cruz Biotechnology. Antibodies to FASN, SCD1 and ACC were from Cell Signaling. Antibodies to Ser193-ph C/EBPα were purchased from ThermoScientific (cat. PA5-37342). Monoclonal anti–β-actin antibody was from Sigma (St. Louis, MO). Co-immunoprecipitation studies were performed using TrueBlot reagents as previously described (Jin et al., 2013; 2015).

**Protein isolation and Western blotting—**Cytoplasmic and nuclear extracts were isolated from livers of mice as described in previous paper (Wang et al., 2010; Jin et al., 2015). Inhibitors of phosphatases were included in all buffers used for the isolation of proteins or protein-protein complexes. Proteins (50 to 100 μg) were loaded on gradient (4 to 20%) polyacrylamide gels, transferred onto membranes, and probed with antibodies against proteins of interest. To verify protein loading, each filter was re-probed with Abs to β-actin.

**Real Time Quantitative Reverse Transcriptase-PCR—**Total RNA was isolated from mouse livers using RNEasy Plus mini kit (Qiagen). cDNA was synthesized with 2ug of total RNA using a High-Capacity cDNA Reverse Transcription Kit (ThermoFisher). cDNA was diluted five times with DEPC treated water and subsequently used for RT-PCR assays with the TaqMan Gene Expression system (Applied Biosystems). Gene expression analysis was performed using the TaqMan Universal PCR Master Mix (Applied Biosystems) in a total volume of 10μl containing 5μl Master Mix, 1.5μL water, 3μl cDNA template and 0.5μl of the gene-specific TaqMan Assay probe mixture. The cycling profile was 50°C for 2 minutes, 95°

for 10 minutes followed by 40 cycles of 95°C for 15 seconds and 60°C for 1 minute as recommended by the manufacturer. TaqMan probe mixture for FXR (Mm00484523_m1), Gankyrin (Mm00450376_m1) and β-Actin (Mm02619580-g1) purchased from Applied Biosystems. All results were normalized to β-Actin. Amplification and quantification were done with the Applied Biosystem StepOne Plus RT-PCR System.

**Statistical Analysis—**All values are presented as means ± S.D. Statistical analyses were performed using the Student's *t* test. Statistical significance was assumed when *, $p < 0.05$ and **, $p<0.01$.

## Supplementary Material

Refer to Web version on PubMed Central for supplementary material.

## Acknowledgments

This work is supported NIH grants R01DK102597 and R01CA159942 (NT), by NIH grants AR052791, AR064488 (LT) and by Internal Development Funds from CCHMC (NT, LT). We thank Taeko Noah and Mary McKay for their assistance in experiments with mice and Holly Poling for help with immunostaining.

## References

Anders L, Ke N, Hydbring P, Choi YI, Widlund HR, Chick JM, Zhai H, Vidal M, Gygi S, Braun P, Sicinski P. A systematic screen for cdk4/6 substrates links FOXM1 phosphorylation to senescence suppression in cancer cells. Cancer Cell. 2011; 20:620–634. [PubMed: 22094256]

Baker SJ, Reddy FE. CDK4: A key player in the Cell Cycle, Development and Cancer. Genes & Cancer. 2013; 3:658–669.

Carr RM, Reid AE. FXR agonists as therapeutic agents for non-alcoholic fatty liver disease. Curr Atheroscler Rep. 2015 Apr.17(4):500. [PubMed: 25690590]

Cohen CJ, Horton JD, Hobbs HH. Human Liver Disease: old questions and new insights. Science. 2011; 332:1519–1523. [PubMed: 21700865]

Dickson MA, Schwarz GK. Development of cell-cycle inhibitors for cancer therapy. Current Oncology. 2009; 16:36–43.

Endicott J, Noble NE, Tucker JA. Cyclin-dependent kinases: inhibition and substrate recognition. Curr Opin Struct Biol. 1999; 9:738–744. [PubMed: 10607671]

Flaherty KT, Lorusso PM, Demichele A, Abramson VG, Courtney R, Randolph SS, Shaik MN, Wilner KD, O'Dwyer PJ, Schwarz GK. Phase I, dose-escalation trial of the oral cyclin-dependent kinase 4/6 inhibitor PD 0332991, administered using a 21-day schedule in patients with advanced cancer. Clin Cancer Res. 2012; 18:568–576. Epub 2011 Nov 16. [PubMed: 22090362]

Fleet T, Zhang B, Lin F, Zhu B, Dasgupta S, Stashi E, Tackett B, Thevananther S, Rajapakshe KI, Gonzales N, Dean A, Mao J, Timchenko N, Malovannaya A, Qin J, Coarfa C, DeMayo F, Dacso CC, Foulds CE, O'Malley BW, York B. SRC-2 orchestrates polygenic inputs for fine-tuning glucose homeostasis. Proc Natl Acad Sci U S A. 2015 Oct 20. 2015 pii: 201519073. [Epub ahead of print].

Gil J, Peters G. Regulation of INK4β–Arf-INK4α tumor suppressor locus: all for one and one for all. Nat Rev Mol Cell Biol. 2006; 7:667–677. [PubMed: 16921403]

Hebbard L, George J. Animal models of nonalcoholic fatty liver disease. Gastroenterology and Hepatology. 2011; 8:34–44.

Hill-Baskin AE, Markievski MM, Bucher DA, Shao H, DeSantis D, Hsiao G, Subramaniam S, Berger NA, Croniger C, Lambris J, Nadeau JH. Diet-induced hepatocellular carcinoma in genetically predisposed mice. Hum Mol Gen. 2009; 18:2975–2988. [PubMed: 19454484]

Jiang Y, Iakova P, Jin J, Sullivan S, Sharin V, Hong I-W, Anakk S, Major A, Darlington G, Finegold M, Moore D, Timchenko NA. FXR inhibits gankyrin in mouse livers and prevents development of liver cancer. Hepatology. 2013; 57:1098–1106. [PubMed: 23172628]

Jin J, Hong IH, Lewis K, Iakova P, Breaux M, Jiang Y, Sullivan E, Jawanmardi N, Timchenko L, Timchenko NA. Cooperation of C/EBP family proteins and chromatin remodeling proteins is essential for termination of liver regeneration in mice. Hepatology. 2015; 6:315–325.

Jin J, Iakova P, Wang G-l, Shi X, Haefliger S, Finegold M, Timchenko NA. Epigenetic changes play critical role in age-associated dysfunction of the liver. Aging Cell. 2010; 9:895–910. [PubMed: 20698834]

Jin J, Iakova P, Breaux M, Sullivan E, Jawanmardi N, Chen D, Jiang Y, Medrano EE, Timchenko NA. Increased expression of enzymes of triglyceride synthesis is essential for the development of hepatic steatosis. Cell Reports. 2013; 3:831–843. [PubMed: 23499441]

Johnson PE. Molecular stop signs: regulation of cell-cycle arrest by C/EBP transcription factors. J Cell Science. 2005; 118:2545–2555. [PubMed: 15944395]

Leonard JP, LaCasce AS, Smith MR, Noy A, Chirieac LR, Rodig SJ, Yu JQ, Vallabhajosula S, Schoder H, English P, Neuberg DS, Martin P, Millenson MM, Ely SA, Courtney R, Shaik N, Wilner KD, Randolph S, Van den Abbele AD, Chen-Kiang SY, Yap JT, Shapiro GI. Selective CDK4/6 inhibition with tumor responses by PD0332991 in patients with mantle cell lymphoma. Blood. 2012; 119:4597–4607. Epub 2012 Mar 1. [PubMed: 22383795]

Luke JJ, D'Adamo DR, Dickson MA, Keohan ML, Carvajal RD, Maki RG, de Stanchina E, Musi E, Singer S, Schwartz GK. The cyclin-dependent kinase inhibitor flavopiridol potentiates doxorubicin efficacy in advanced sarcomas: preclinical investigations and results of a phase I dose-escalation clinical trial. Clin Cancer Res. 2012; 18:2638–2647. [PubMed: 22374332]

Nagaria TS, Williams JL, Leduc Ch, Squire JA, Greer P, Sangrar W. Flavopiridol synergizes with Sorafemib to induce cytotoxicity and potentiate antitumorigenic activity in EGFR/HER2 and mutant RAS/RAF breast cancer model systems. Neoplasia. 2013; 8:939–951.

Rivadeneira DB, Mayhew CN, Thangavel C, Sotillo E, Reed CA, Grana X, Knudsen E. Proliferative suppression by cdk4/6 inhibition: complex function of the RB-pathway in liver tissue and hepatoma cells. Gastroenterology. 2010; 138:1920–1930. [PubMed: 20100483]

Schmucker DL. Age-related changes in liver structure and functions: Implications for disease? Exp Gerontol. 2005; 40:650–659. [PubMed: 16102930]

Timchenko NA. Aging and liver regeneration. Trends in Endocrinol and Metabol. 2009; 20:171–176.

Timchenko NA. Senescent Liver. In: Monga SPS, editorMolecular Pathology of the Liver Diseases. Springer Science + Business Media, LLC; 2011. PP279–PP290. DOI10/978- 14419-7107-4_19,@

VanSaun MN, Mendonsa AM, Gorden DL. Hepatocellular proliferation correlates with inflammatory cell and cytokine changes in a murine model on nonalcoholic fatty liver disease. PLOS One. 2013; 8:e73054. [PubMed: 24039859]

Wang G-L, Shi X, Salisbury E, Sun Y, Albrecht JH, Smith RG, Timchenko NA. Cyclin D3 maintains growth inhibitory activity of C/EBPα by stabilizing C/EBPα-cdk2 and C/EBPα-Brm complexes. Mol Cell Biol. 2006; 26:2570–2582. [PubMed: 16537903]

Wang G-L, Timchenko NA. Dephosphorylated C/EBPα accelerates cell proliferation through sequestering retinoblastoma protein. Mol Cell Biol. 2005; 25:1325–1338. [PubMed: 15684384]

Wang G-L, Shi X, Haefliger S, Jin J, Major A, Iakova P, Finegold M, Timchenko NA. Elimination of C/EBPα through the ubiquitin-proteasome system promotes the development of liver cancer in mice. J Clin Invest. 2010; 120:2549–2562. [PubMed: 20516642]

Xu JY, Li ZP, Zhang L, Ji G. Recent insights into farnesoid X receptor in nonalcoholic fatty liver disease. World J Gastroenterol. 2014; 20:13493–13500. [PubMed: 25309079]

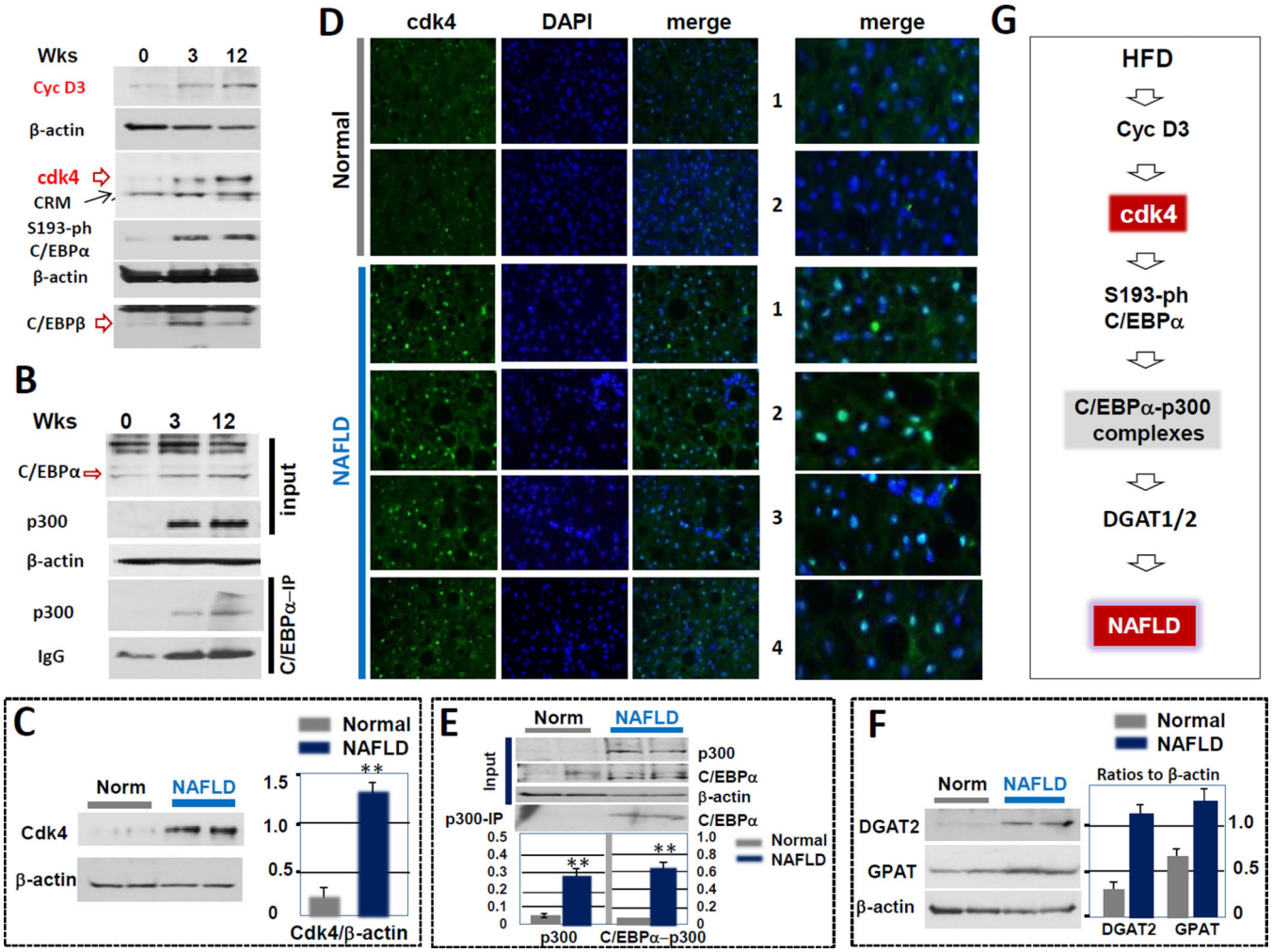


**Figure 1. Cdk4 is activated in animal models of NAFLD and in patients with NAFLD**

**(A)** Cyclin D3/ckd4-C/EBP-p300 pathway is activated in mouse livers after HFD treatment. Western blotting shows that cyclinD3, cdk4, ph-C/EBPα, p300 are increased in livers after HFD treatment. **(B)** C/EBPα-p300 complexes are elevated during development of hepatic steatosis in mice. C/EBPα was immunoprecipitated from nuclear extracts and IPs were examined by Western blotting with antibodies to p300. Upper image shows input of the proteins. IgG; signals of immunoglobulins on the IP membranes. Images on Fig 1A and B represent typical pictures of three independent experiments with three mice at each time point. Examination of additional mice are also shown in Fig 2C. **(C)** Protein levels of cdk4 are increased in livers of patients with fatty liver disease. Western blotting was performed with total protein extracts isolated from the livers. The membrane was re-probed with antibodies to β-actin. Bar graphs show a summary of three independent experiments. **(D)** Immunostaining of normal livers and livers from 4 patients with fatty liver diseases using antibodies to cdk4. The slides were stained with DAPI. The right panel shows enlarged pictures of merged images. **(E)** Protein levels of p300 and C/EBPα-p300 complexes are increased in livers of patients with fatty liver disease. Upper image: Western blotting was performed with total protein extracts isolated from the livers. The membrane was re-probed

with antibodies to β-actin. Bar graphs show calculations of p300 and C/EBPα-p300 complexes as ratios to β-actin. **(F)** Amounts of DGAT2 and GPAT are increased in livers of patients with fatty liver diseases. Western blotting was performed with total protein extracts isolated from the livers. The membranes were re-probed with antibodies to β-actin. Bar graphs show levels of GPAT and DGAT1 as ratios to β-actin. **(G)** A model showing hypothetical mechanisms for the development of NAFLD (see text).

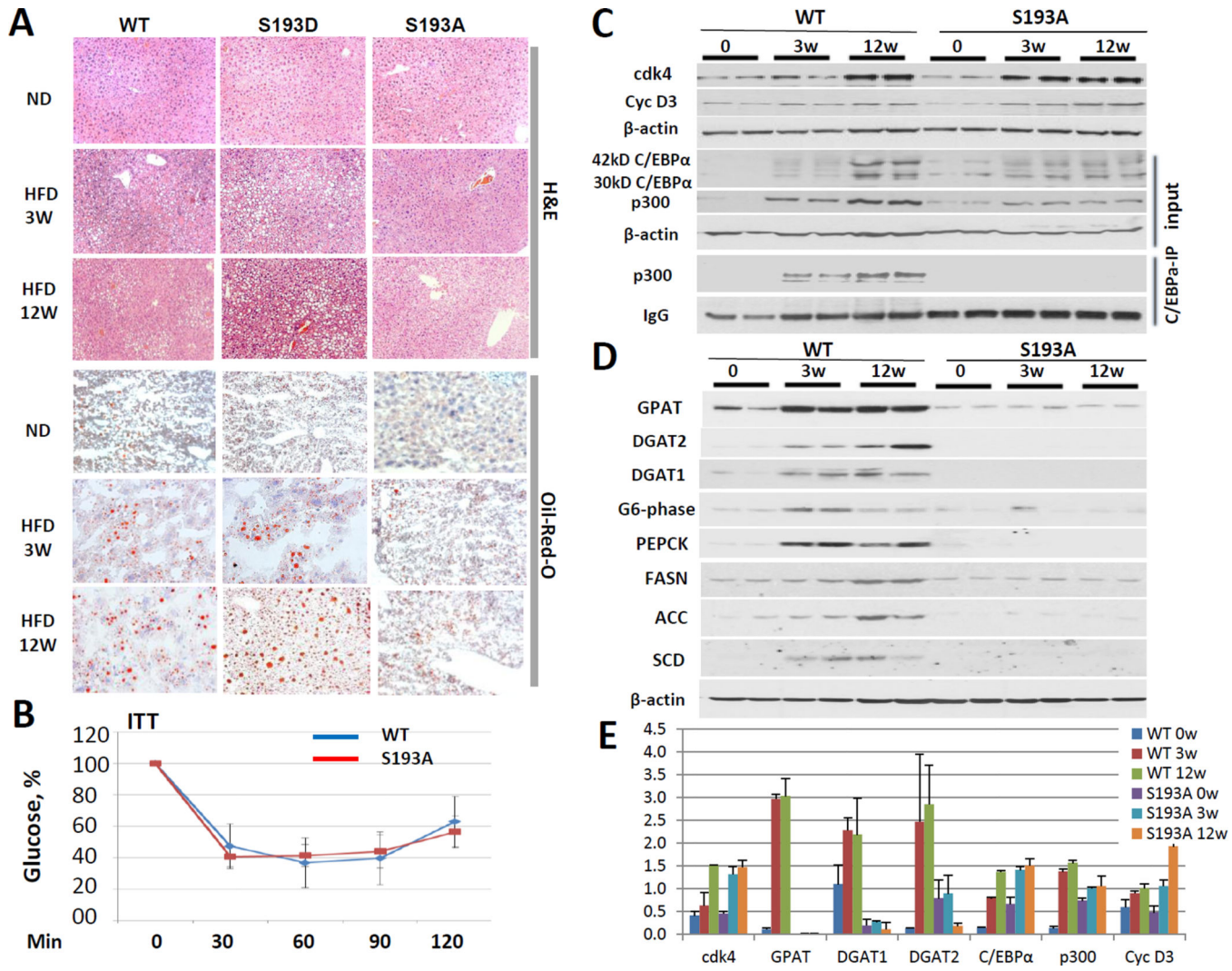


**Figure 2. Cdk4-resistant C/EBPα-S193A mice do not develop hepatic steatosis under conditions of HFD protocol**

**(A)** S193A mice do not develop hepatic steatosis, while S193D mice are developing hepatic steatosis much faster than wild type mice after 3 weeks and 12 weeks of HFD conditions. A typical picture of H&E and Oil-Red O staining of WT, S193D and S193A livers (five mice of each genotype) is shown in three and 12 weeks after initiation of HFD. Scale bar: 40 μm. **(B)** Insulin-dependent lowering of glucose is not affected in S193A mice. Insulin Tolerance Test was performed with WT and S193A mice as shown in Supplement Materials. **(C)** Cyclin D3-cdk4 pathway is identically elevated in WT and S193A mice, but C/EBPα-p300 complexes are not formed in livers of S193A mice. Western blotting was performed with antibodies to cdk4, cyclin D3, C/EBPα and p300. **Bottom image:** C/EBPα was immunoprecipitated from nuclear extracts and p300 was examined in these IPs. IgG, signals of immunoglobulins detected on the membrane. **(D)** Expression of enzymes of TG synthesis, glucose synthesis and lipid metabolism. Cytoplasmic extracts from WT and S193A mice were probed with antibodies shown on the left. Membranes were re-probed with antibodies to β-actin. **(E)** Levels of proteins on Fig 2C and D were calculated as ratios to β-actin. The

bar graphs show a summary three repeats with three mice per each time point. Additional calculations are shown in Supplemental Figure 2.

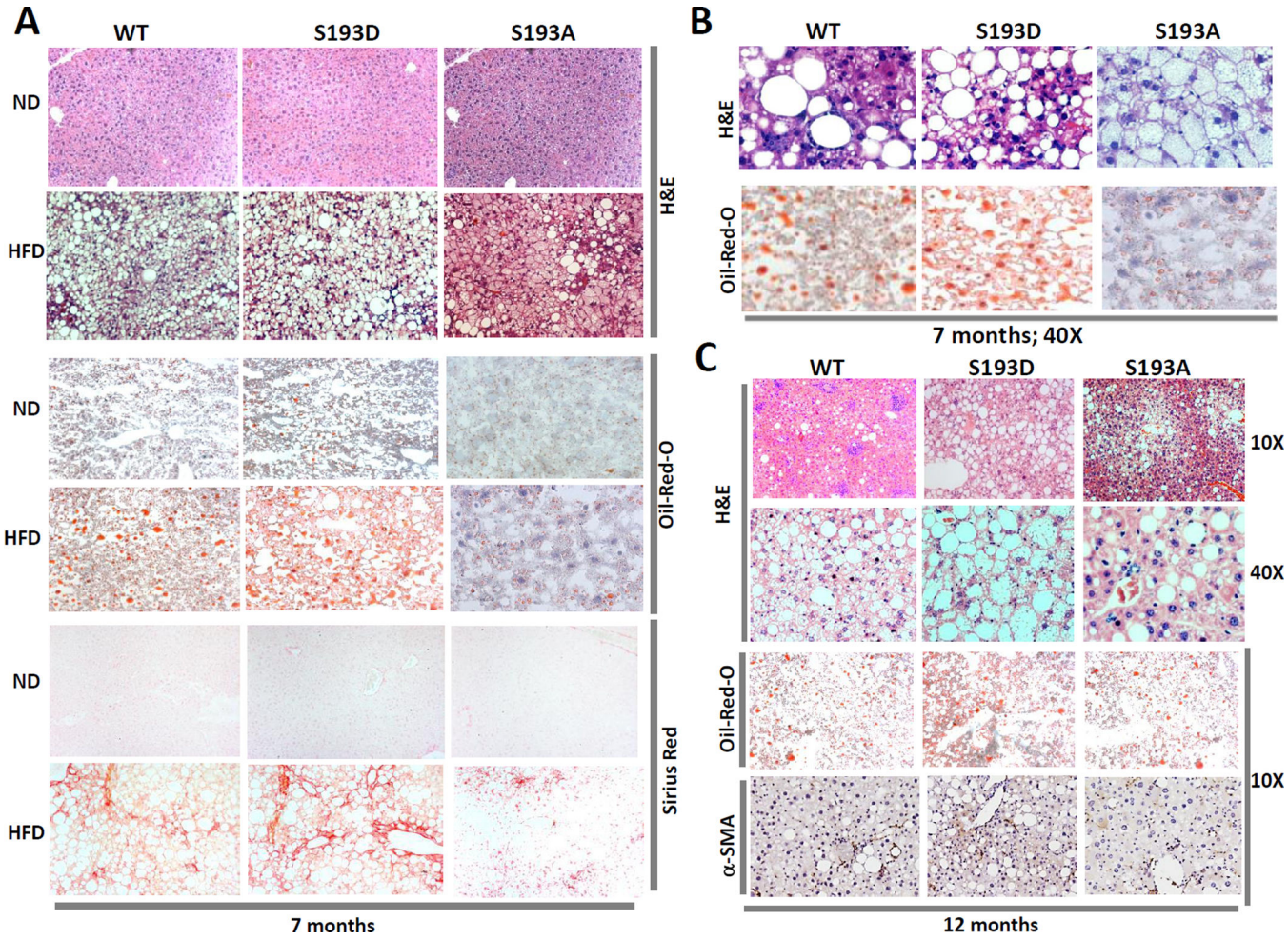


**Figure 3. Development of NAFLD and fibrosis is inhibited in S193A mice after 7 and 12 months of HFD treatments**

**(A)** A typical pictures of H&E, Oil-Red-O and Sirius Red stinging of WT, S193D and S193A livers under HFD conditions. Upper image shows H&E staining of the livers, middle image shows Oil-Red O staining, bottom image shows Sirius Red staining. Scale bar: 40 μm. **(B)** Sections of H&E staining under high magnification. **(C)** A typical picture of H&E and Oil-Red-O stinging of WT, S193D and S193A livers under 12 months of HFD conditions. Upper image shows H&E staining of the livers and bottom image shows Oil-Red O and α-SMA staining. Scale bar: 40 μm. The figure shows typical pictures obtained with livers of five mice of each genotype.

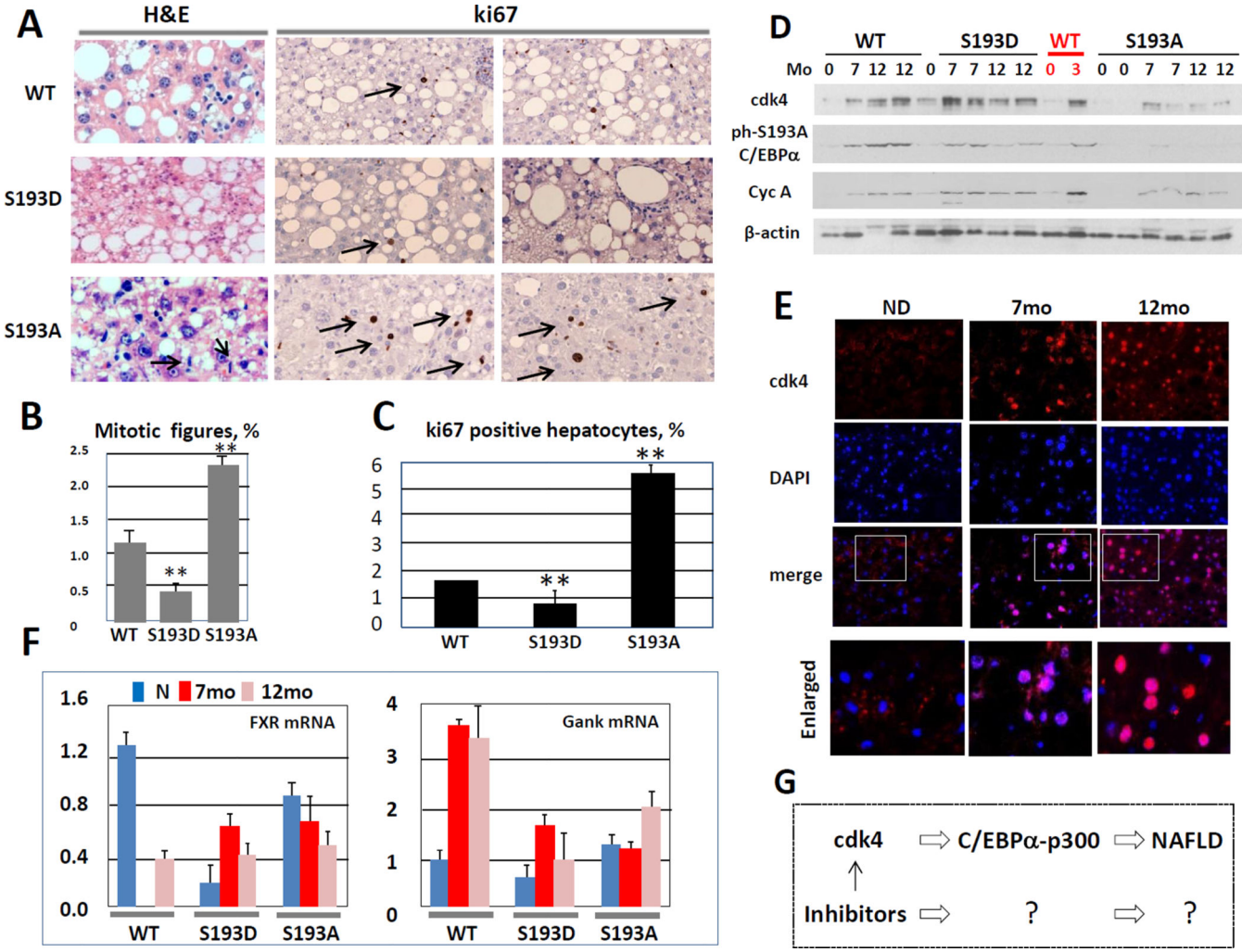


**Figure 4. 12 months treatments with HFD lead to increased liver proliferation and to initiation of cancer-specific FXR-Gank pathway**

**(A)** Left panel: H&E staining shows mitotic figures. Right image shows ki67 staining of livers after 12 months of HFD. **(B)** Bar graphs show number of mitotic figures in WT, S193D and S193A mice per 1,000 hepatocytes. **(C)** Bar graphs show percent of ki67 positive hepatocytes. Three animals of each genotype were used for calculations of mitotic figures and BrdU uptake. **(D)** cdk4-cyclin D3 pathway in WT, S193D and S193A mice at 7 and 12 months after initiation of HFD protocol. Nuclear extracts were isolated from livers and used for Western blotting with Abs shown on the left. **(E)** Amounts of cdk4 are increased in nuclei of hepatocytes after HFD treatment. Liver sections were stained with antibodies to cdk4 and with DAPI. Enlarged images of merged pictures are shown on the bottom. **(F)** Cancer-specific FXR-Gank pathway is activated in WT, S193D and S193A mice after 7 and 12 months of HFD. Expression of FXR and Gankyrin was determined in livers after 7 and 12 months of HFD. Three animals for each genotype were used in these studies. **(G)** A diagram which summarizes examination of mechanisms of NAFLD in genetically modified animal models.

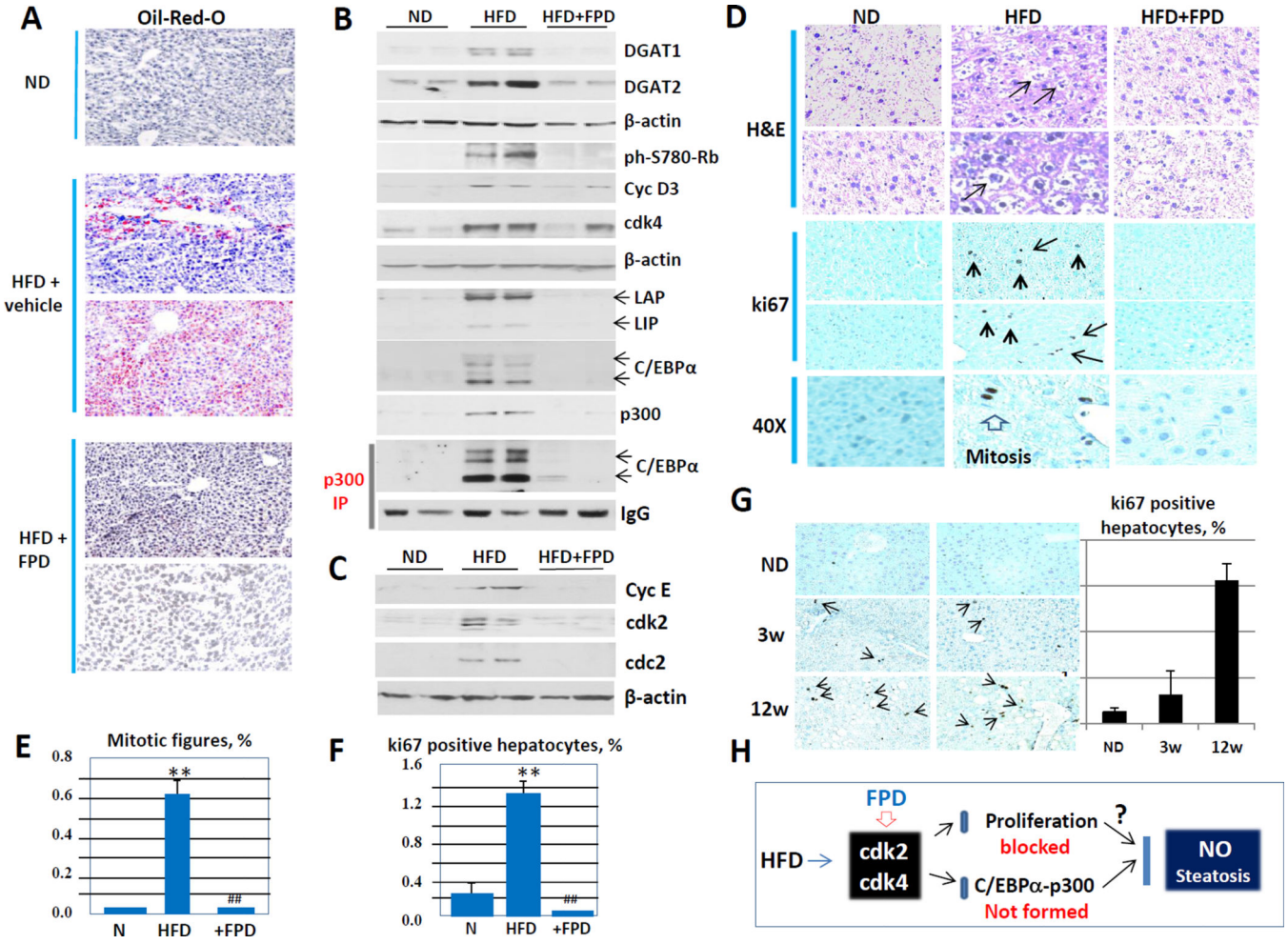


**Figure 5. Inhibition of cdk2/cdk4 activities by flavopiridol prevents development of hepatic steatosis and inhibits liver proliferation**

**(A)** Oil-Red-O staining of livers of mice treated with normal diet, with HFD +vehicle and with HFD +FPD. **(B)** Western blotting of protein extracts with antibodies to enzymes of TG synthesis DGAT1 and DGAT2 and examination of cdk4-C/EBPα pathway in livers of mice treated with HFD and HFD +FPD. Western blotting was performed with Ab shown on the right. LAP and LIP are isoforms of C/EBPβ. Bottom image shows Co-IP studies in which p300 was immunoprecipitated and C/EBPα was examined in these IPs. **(C)** Expression of cell cycle proteins was examined by Western blotting. **(D)** H&E and ki67 staining of livers of mice treated with normal diet (ND), with high fat diet (HFD); and with HFD plus Flavopiridol (HFD+FPD). 40X shows ki67 staining under 40X magnification. **(E)** Percent of mitotic figures. **(F)** % of ki67 positive hepatocytes. Four animals of each group were used for calculations of mitotic figures and ki67 staining. **(G)** Liver proliferation was examined in mice after 3 and 12 weeks of HFD using ki67 staining. Left images show typical pictures of ki67 staining. Bar graphs show % of ki67 positive hepatocytes. **(H)** A diagram summarizing examination of effects of FPD on HFD-mediated steatosis and liver proliferation.

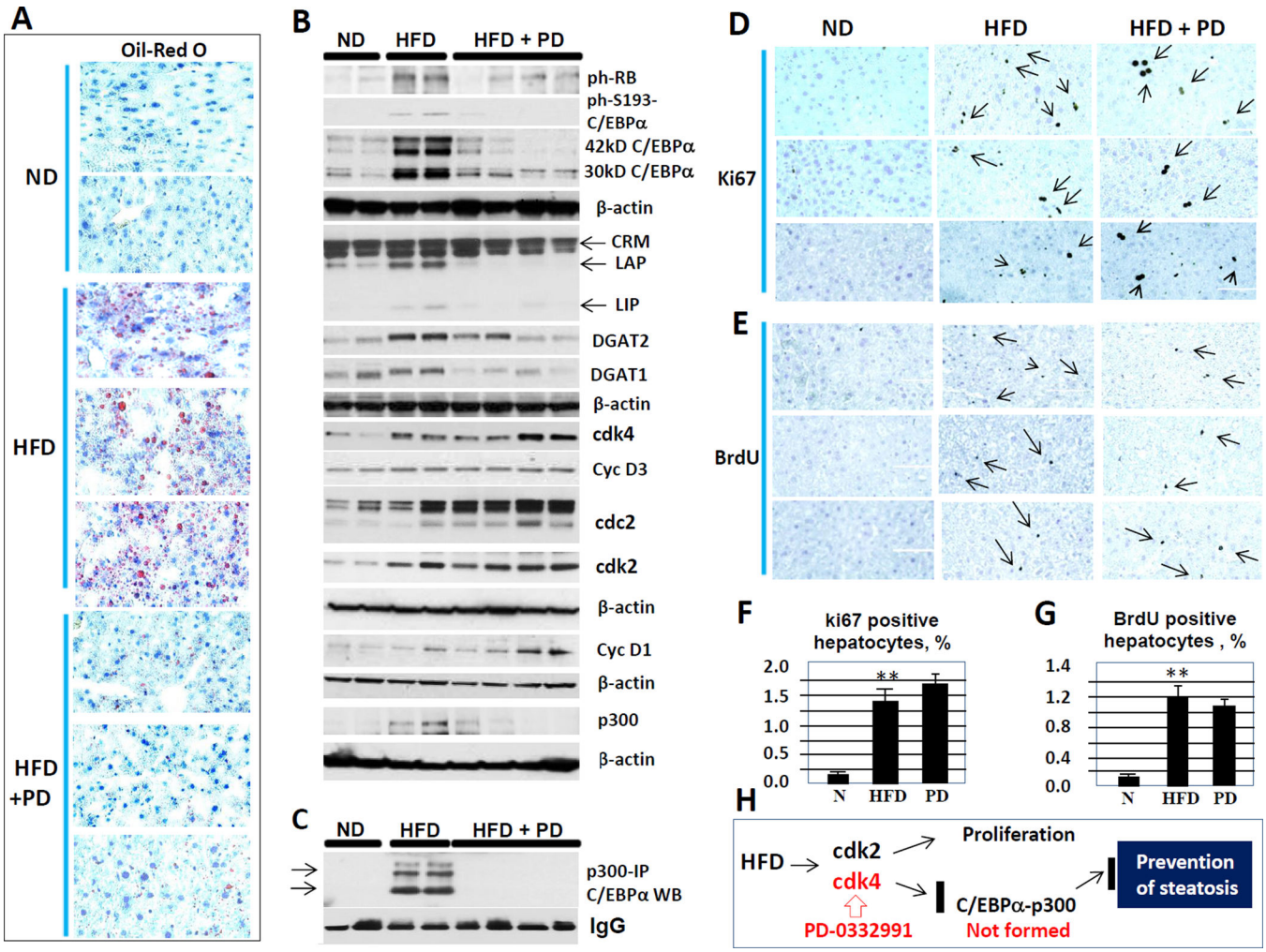


**Figure 6. Inhibition of cdk4 by specific inhibitor PD-0332991 prevents development of steatosis, but does not block liver proliferation**

**(A)** Oil-red-O staining of levers of mice treated with normal diet, with HFD and with HFD + PD-0332991. **(B)** Western blotting with antibodies shown on the right. LAP and LIP are isoforms of C/EBPβ protein. CRM; cross reactive molecule. **(C)** Examination of C/EBPα-p300 complexes by Co-IP approach. **(D and E)** Examination of liver proliferation by ki67 staining and BrdU-uptake. Typical pictures are shown. **(F and G)** Bar graphs show % of ki67 positive and BrdU positive hepatocytes. **(H)** A diagram summarizing examination of effects of PD-0332991 on HFD-mediated steatosis and liver proliferation. Data in this figure show analyses of four-five mice of each group.

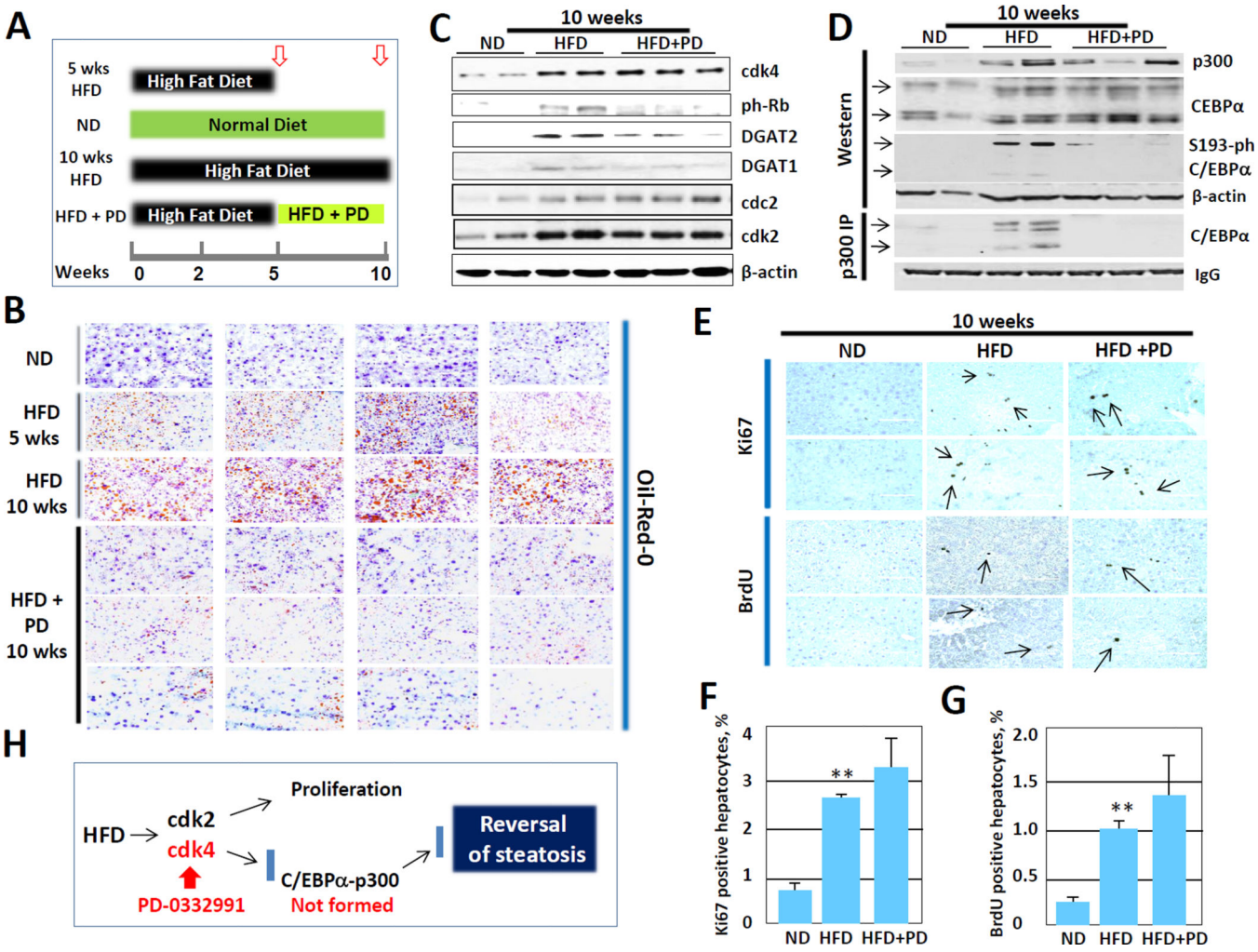


**Figure 7. Inhibition of cdk4 in mice with existing hepatic steatosis dramatically reduces steatosis**

**(A)** A diagram showing the strategy of experiments. **(B)** Oil-Red-O staining of livers. Typical pictures of 4 mice per each group are shown. **(C)** Inhibition of cdk4 activity by PD-0332991 and expression of DGAT1 and DGAT2 proteins. Western was performed with Abs shown on the right. **(D)** Inhibition of cdk4 activity by PD-0332991 reduces amounts of C/EBPα-p300 complexes. Input: Western blotting with Abs to C/EBPα and p300 showing expression and input of these proteins. P300-IP: examination of p300 immunoprecipitates by Western blotting with Abs to C/EBPα. 42kD and 30kD C/EBPα isoforms are shown by arrows. **(E)** Typical pictures of ki67 staining and BrdU uptake. **(F and G)** % of ki67 positive and BrdU positive hepatocytes was calculated. Bar graphs represent summary of analyses of five mice per each group. **(H)** A diagram showing the results of reversion of HFD-mediated steatosis by PD-0332991-mediated inhibition of cdk4.